DEVELOPMENT OF JT-60SA EQUILIBRIUM CONTROLLER WITH AN IMPROVED ISO-FLUX METHOD AND VERTICAL DISPLACEMENT EVENTS PREDICTOR

ID: 821

S. Inoue, Y. Miyata, H. Urano, T. Suzuki, T. Wakatsuki, M. Yoshida, A. Matsuyama, N. Aiba
T. Bando, M. Takechi, S. Ide, and the JT-60SA team
National Institutes for Quantum and Radiological Science and Technology
inoue.shizuo@qst.go.jp

ABSTRACT

- To resolve concerns for heat/electromagnetic loads from vertical displacement events (VDEs), we developed an equilibrium controller, which can predict and control VDEs to an arbitrary direction and allows us to cope with either upward or downward unmitigated VDEs. Here we improve the prediction rate by parameterizing a power supplies voltage saturation rate with a newly developed adaptive voltage allocation (AVA) scheme.
- Furthermore, the AVA scheme also broadens accessible elongation by 0.3 in the presence of power supplies voltage saturation due to hybrid plasma current and shape/position control and unknown plasmas disturbances.
- In preparation for coming JT-60SA integrated commissioning, the VDE predictor and the AVA scheme are implemented in our equilibrium controller, and its performance is demonstrated by using "MECS" (Fig. 1).

BACKGROUND

- $\sqrt{\text{fusion output}} \propto$ Plasma pressure $\propto I_p \propto 1+\kappa^2$ when fixing machine unique parameters, e.g., toroidal field, machine size, etc. [Troyon 84, ITER PB 1 (OV)]
  - For fusion output, hybrid control of I_p and VDE is required
- Device conditions of DEMO and JT-60SA (during the integrated commissioning, Fig. 1) for VDE control are highly disparate from present day tokamaks and even from ITER, such as the absence of in-vessel coils, a large gap between plasmas and vacuum vessels, and eddy currents flowing in the breeding blanket (DEMO)
  - W (gap)/ R(major radius) = 0.12 (ITER), ~0.18 (DEMO), 0.2 (JT-60SA comm.)
- Disruption prevention including VDEs has been extensively explored [e.g., Strait 19], but it may still not be easy to mitigate all disruptions perfectly, which requires forecasting disruptions before delay time of actuators

NEWLY DEVELOPED CONTROL SCHEME

Adaptive Voltage Allocation (AVA) scheme [submitted to NF]

AVA scheme achieves hybrid control of the P/S and the I_p under power supply voltage limits

Position/shape & I_p control

$$\delta\psi_S = \psi_X - \psi_S$$
$$\delta\psi_X = \psi_{X,\mathrm{new}} - \psi_X = -L_i(I_{p,\mathrm{ref}} - I_p)$$

ISO-FLUX control : diff. btw. LCFS and control points (P/S) and its offset (I_p)

+PID

PID control

$$\delta\boldsymbol{\psi}_{S,\mathrm{PID}} = G_S\left\{G_{SP}\delta\psi_S + G_{SI}\int\delta\psi_S dt + G_{SD}\frac{\partial\psi_S}{\partial t}\right\}$$
$$\delta\boldsymbol{\psi}_{X,\mathrm{PID}} = G_X\left\{G_{XP}\delta\psi_X + G_{XI}\int\delta\psi_X dt + G_{XD}\frac{\partial\psi_X}{\partial t}\right\}$$

(P-term, I-term, D-term)

- Gains are optimized by frequency response analyses
- G_X: for control, reduces influence of $\delta\psi_X$ control on $\delta\psi_S$ control
- G_S : for monitor, VDE prediction

Automatic gain control

1st: $\delta\boldsymbol{\psi} = \delta\psi_{X,\mathrm{PID}}$ — Loop — G_X w/o V_C saturation — 2nd — 3rd: $\delta\boldsymbol{\psi} = \delta\boldsymbol{\psi}_{S,\mathrm{PID}} + \delta\boldsymbol{\psi}_{X,\mathrm{PID}}$ ($G_{S,\mathrm{AVA}} = 1$)

Control & Circuit equation

$$\delta\boldsymbol{I}_C = \boldsymbol{M}^{\dagger}\delta\boldsymbol{\psi}$$
$$\boldsymbol{M}_{CC}\frac{\partial \boldsymbol{I}_C}{\partial t} + \frac{\partial(\boldsymbol{M}_{PC}I_p)}{\partial t} + \boldsymbol{R}\boldsymbol{I}_C = \boldsymbol{V}_C$$

I_C: Coil currents
M_{CC}: mutual inductance of coils
M_{PC}: mutual inductance btw plasma and coils
R: Coil resistance
I_p: Plasma current

$\boldsymbol{V}_C$ (e.g., 10 coil voltages for SA) ⇨ Power supplies

VDE Prediction scheme

Control cycle in JT-60SA: 250 μs

- VDE control to an arbitrary direction could halve the concerns to protect the device from either upward or downward VDEs: one divertor side of MGI/SPI is sufficient?
- VDE Predictor: a support vector machine (SVM) classifier with three parameters: vertical velocity ($v_{Z,\mathrm{ax}}$), decay index (n-index), newly introduced gain ($G_{S,\mathrm{AVA}}$)
- SVM is trained by 17 simulation with 7 upward VDEs and 378/460747 trained/test data

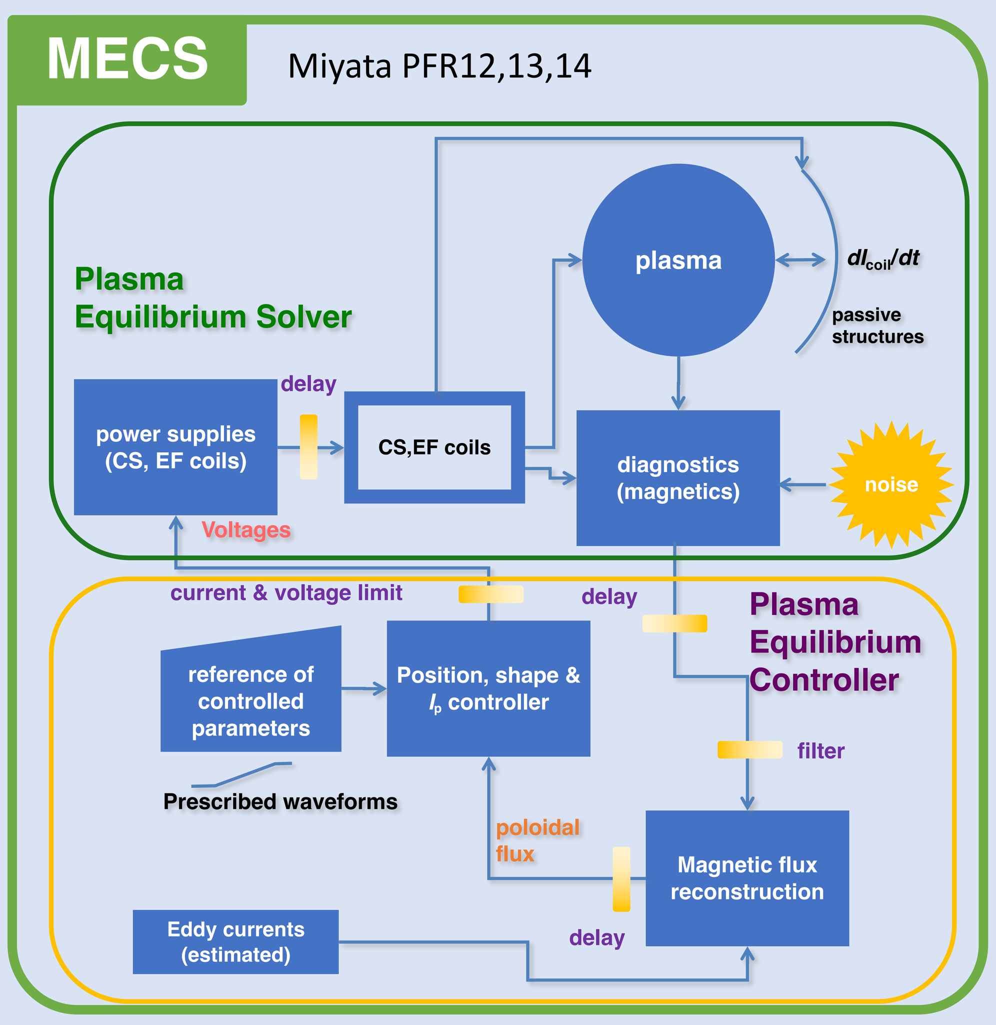

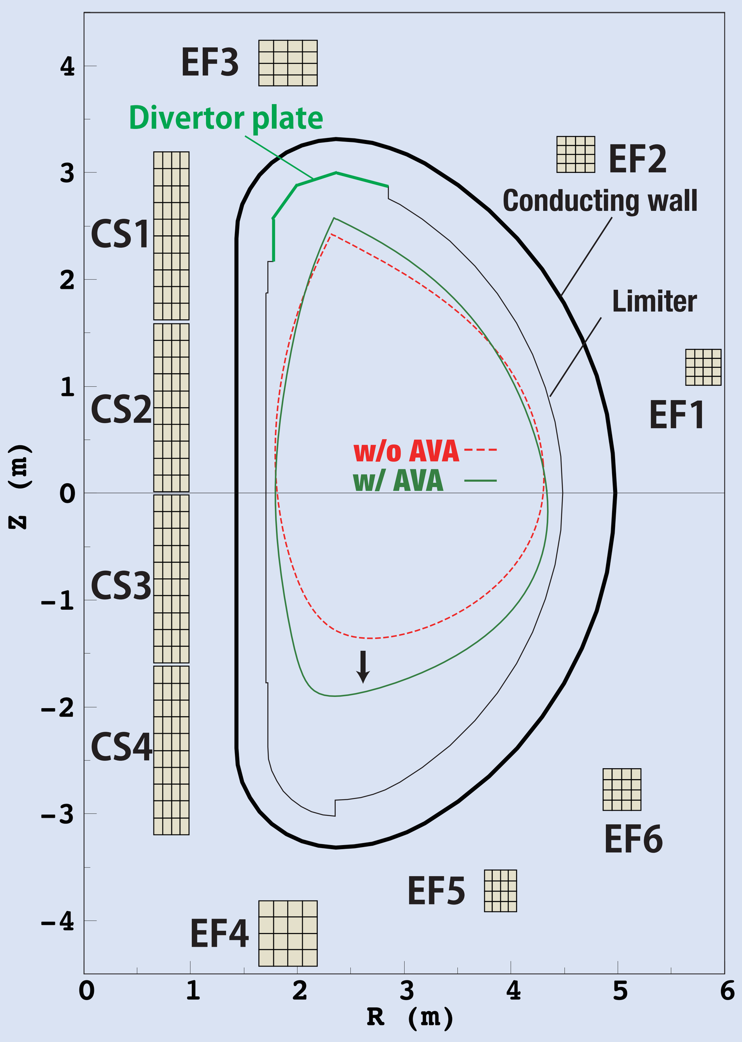

Fig. 1. Schematic view of MECS and JT-60SA during integrated commissioning

EFFECT of AVA: Accessible κ is broadened in JT-60SA

- I_p-collapse is simulated at t = 6 s, during I_p ramp-up from 1->2.5 MA, which not only affects I_p but also VDE control (Fig. 2a,e,f)
- Comparison btw w/ and w/o AVA clearly shows that VDE is successfully suppressed by adjusting $G_{X,\mathrm{AVA}}$ even with higher κ (Fig. 2b,c,d)

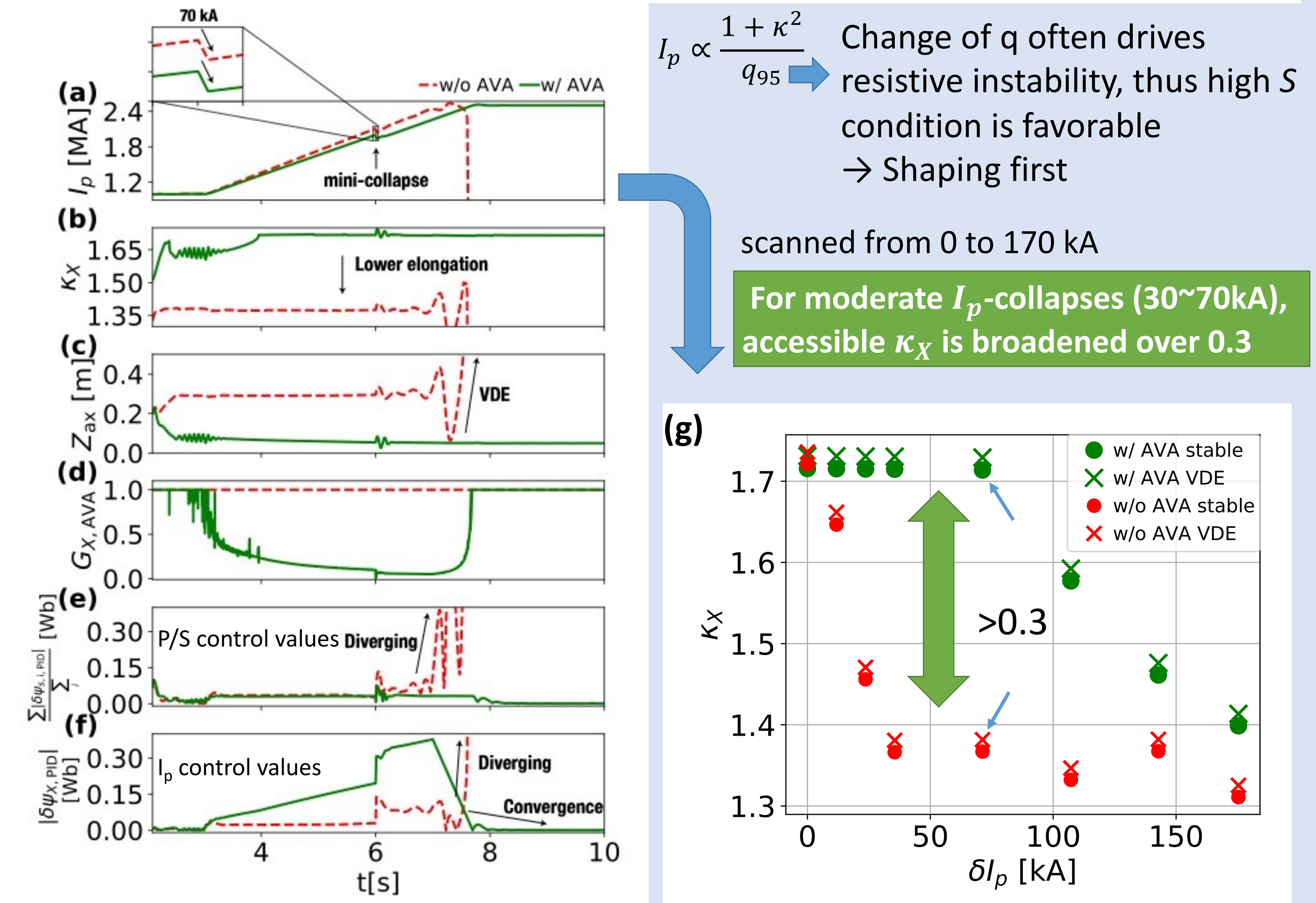

Fig. 2. Temporal evolution of (a) I_p, (b) κ_X, (c) vertical position of magnetic axis, (d) $G_{X,AVA}$, and the averaged controlled values of (e) P/S, (f) I_p, and (g) its scan

TEST of VDE DIRECTION CONTROL SCHEME in JT-60SA

- Typical VDE follows up/down oscillation due to the control
- Original downward VDE is controlled to upward (Fig. 3bc)
- For precise VDE prediction, we should evaluate performance of controller, where prediction by n and $v_{Z,\mathrm{ax}}$ causes false alarms but is improved by $G_{S,\mathrm{AVA}}$

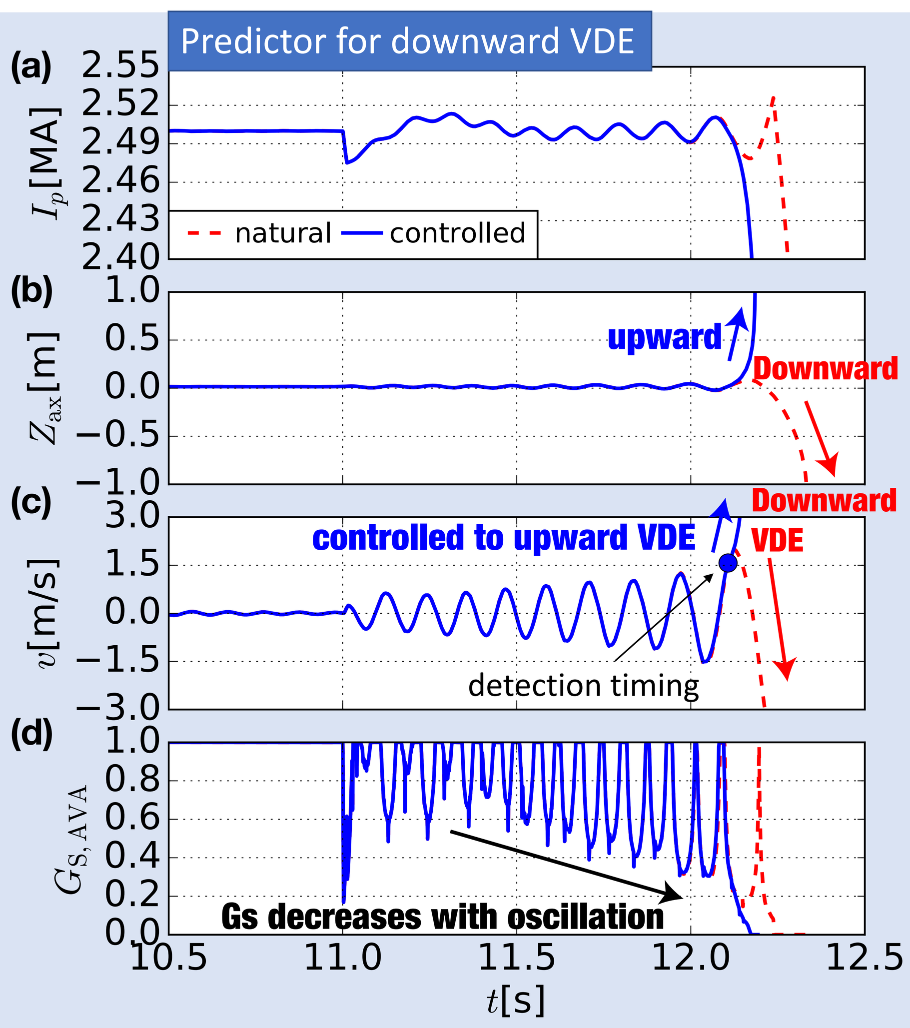

Fig. 3. Temporal evolution of (a) I_p, (b) vertical position, (c) $v_{Z,\mathrm{ax}}$, and (d) $G_{S,\mathrm{AVA}}$

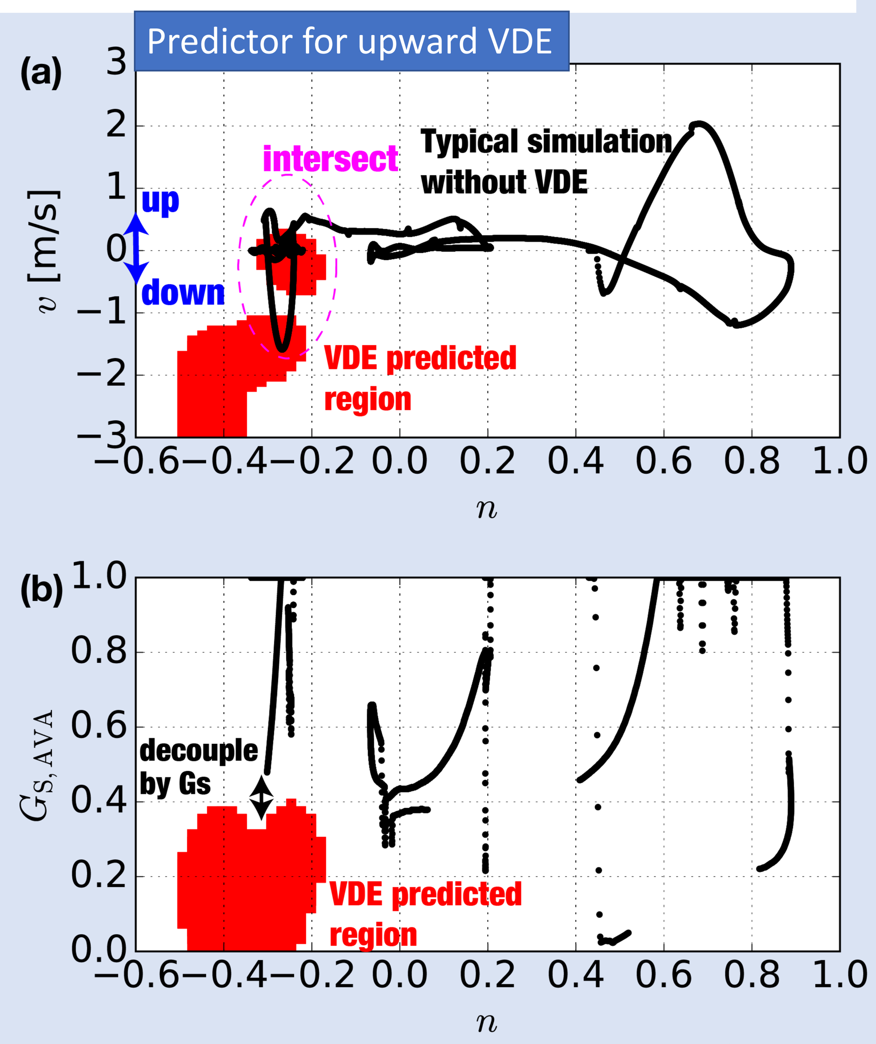

Fig. 4. VDE predicted region (filled), which are projected to (a) (n,v) and (b) (n, $G_{S,AVA}$) plane. Typical simulation data without VDE are also shown by dot points.

CONCLUSION

- An advanced ISO-FLUX control scheme as well as VDE control scheme is developed and implemented in the JT-60SA equilibrium controller
- An accessible κ_X is broadened by 0.35 in the presence of the moderate Ip mini-collapse (30 ~ 70 kA in JT-60SA)
- New logic guides the VDE to an arbitrary direction and could halve the concerns to protect the device from either up/downward VDEs
- $G_{S,\mathrm{AVA}}$ improves false alarm rates for the VDE detection

ACKNOWLEDGEMENTS

- This research was supported by Grant-in-Aid for Young Scientists (Grant No. 19K14696).